Comparison of Renewable Large-Scale Energy Storage Power Plants Based on Technical and Economic Parameters

Ann-Kathrin Klaas[✉] and Hans-Peter Beck

Institute of Electrical Power Engineering and Energy Systems,
Clausthal University of Technology, Clausthal-Zellerfeld, Germany
`ann-kathrin.klaas@tu-clausthal.de`

Abstract. With the increasing expansion of renewable energies in Germany, the temporary electricity surplus is rising and with it the need for large-scale energy storage. In this research, a systematic comparison of different concepts for large-scale storage of electrical energy is carried out based on technical and economic parameters. The investigated concepts include a diabatic compressed air energy storage power plant (CAES), an adiabatic compressed air energy storage power plant (ACAES), a hydrogen compressed air energy storage power plant (HCAES) as well as a hydrogen energy storage power plant with a gas turbine (HES-GT) and a hydrogen storage power plant with a fuel cell (HES-FC).

The round-trip efficiency and the storage capacity of each storage power plant concept are determined using simplified thermodynamic correlations. The charging capacities range between 3.9 GWh (CAES) and 81.8 GWh (HES) with round-trip efficiencies from 28% (HES-GT) to 69% (ACAES). The technology readiness level is estimated between 8 (CAES) and 4 (ACAES). The investment costs of each component are determined with cost functions based on thermodynamic parameters and an extensive literature review. The analysis additionally includes the ability to provide ancillary services, greenhouse gas emissions, storage losses and demand of land. Results show that the hydrogen compressed air energy storage (HCAES) is the best storage option when all criteria are weighted equally. CAES is not suitable for a renewable energy system due to carbon emissions and ACAES and HES-FC both have a low TRL and high investment costs. However, all energy storage concepts have different advantages and development potential and the suitability of any concept depends on the use case.

Keywords: large-scale energy storage · compressed air energy storage · hydrogen energy storage · efficiency · storage capacity

1 Introduction

With the increasing expansion of renewable energies to reduce greenhouse gas emissions in Germany, the temporary electricity surplus is rising and with it

Table 1. Nomenclature or symbols and indexes.

Symbol	Description	Symbol	Description	Index	Description	Index	Description
A	area	T	temperature	A	air	H	hydrogen
C	costs	V	volume	C	compressor	HE	heat exchanger
c_P	spec. heat capacity	W	work/energy	CC	combustion chamber	HP	high pressure
$m, \dot{m}$	mass (flow)	β	pressure ratio	ch	charging	LP	low pressure
P	electrical power	ϵ	effectiveness	dch	discharging	R	recuperation
p	pressure	η	efficiency	E	electrolysis	SC	salt cavern
Q	heat	κ	heat capacity ratio	FC	fuel cell	T	turbine
R	spec. gas constant	ρ	density	G	generator	TS	thermal storage

the need for energy storage. Besides small-scale, residential storage systems and short-term balancing storage systems, the need for large-scale, long-term energy storage rises in correlation with the share of renewable energy in the energy system. A study by Agora Energiewende found that a combination of 7 GW of short-term storage and 16 GW of long-term storage poses the highest savings potential in an energy system with 90% renewable energy in Germany [1]. A more recent study suggests 50 GW of battery storage and 7 GW of pumped hydropower storage for a 100% renewable energy system in Germany (full report of [2]) (Table 1).

Energy storage technologies are often classified with regard to the ratio of energy and power. Technologies with a discharging duration of less than 24 h are considered short-term storage systems and are also characterized by high cycle numbers and high cycle efficiencies. A discharging duration of 24 h and more as well as low cycle number and low cycle efficiencies are criteria of long-term storage [3, Chap. 2]. Batteries, pumped hydropower and compressed air energy storage are often considered short-term storage systems, whereas hydrogen storage is considered a long-term storage option [3, Chap. 2]. However, for compressed air energy storage, the sizing of power and storage capacity do not depend on each other. High storage capacities and a comparably low discharging power can lead to discharging durations greater than 24 h (as it is shown later in this paper).

The evaluation and comparison of energy storage concepts has been widely investigated in literature. Klumpp [4] compares pumped hydropower, adiabatic compressed air and hydrogen energy storage based on efficiency, storage capacity and specific investment costs. Blanco et al. [5] gives a review of over 60 studies on the role of long-term energy storage in future energy systems. Yu et al. [6] conduct a comparison of pumped hydropower, compressed air, hydrogen energy storage and heat storage for improving wind power integration. Several medium-scale energy storage concepts with 100 kW discharging power such as pumped hydropower, compressed air, hydrogen and batteries are analysed based on the energy and exergy efficiency in [7]. Schmidt et al. [8] project the future levelized cost of storage for pumped hydro, compressed air, flywheel, different battery technologies, hydrogen and supercapacitors. Zakeri et al. [9] give a comparative life cycle cost analysis of electrical energy storage systems such as pumped

hydrogen, compressed air, batteries and hydrogen. Pérez et al. [10] conduct a life cycle assessment of large-scale underground storage concepts. The carbon footprint of energy storage concepts including hydrogen, compressed air and batteries is calculated in [11]. Astiaso Garcia at al. [12] analyze the potential of hydrogen storage in Europe based on potential locations, excess renewable energy and regulatory frameworks. Budt at al. [13] classify and compare different compressed air energy storage concepts including diabatic, adiabatic an isothermal. Luo et al. [14] give an overview of current developments within compressed air energy storage concepts. In [15], different compressed air energy storage concepts are discussed based on recent advances in materials and other development efforts. Yu et al. [16] analyze the influence of different thermodynamic parameters on the performance of a compressed air energy storage power plant. Safaei et al. [17] conduct a thermodynamic analysis of three compressed air energy storage concepts (diabatic, adiabatic and hydrogen-fueled with a high-temperature electrolysis system). Barbour et al. [18] give a review of adiabatic compressed air energy storage research and discuss the challenges of commissioning such a plant.

To the authors' knowledge, a systematic comparison of large-scale energy storage systems based on both technical and economic criteria with uniform input parameters has not been done yet. Within this research, it is attempted to compare five large-scale, long-term energy storage concepts based on the storage of a gaseous medium in underground salt caverns. Pumped hydro storage and batteries are not included within this comparison. Pumped hydro storage is severely limited by geological conditions [5] and is considered a short-term storage technology with a few exceptions in Norway and the Alps [3, Chap. 2]. The average discharging time of different battery technologies does not exceed 10 h and existing stationary battery storage systems do not surpass a capacity of 100 MWh and a nominal power of 50 MW [19].

The paper has the following structure: Sect. 2 gives an overview of large-scale energy storage concepts and their components. Input parameters are described in Sect. 3 and criteria for comparison are defined in Sect. 4. The results are analyzed in Sect. 5. Results are compared to literature values of the analyzed concepts, lithium-ion batteries and pumped hydropower energy storage. The results are discussed in Sect. 6 and Sect. 7 presents the conclusions. Detailed formulae for the thermodynamic calculations are presented in the appendix.

2   Concepts of Large-Scale Energy Storage Power Plants

A diabatic compressed air energy storage (CAES) power plant consists, similar to a gas turbine power plant, of a compressor, a combustion chamber, a gas turbine and a synchronous machine. However, a CAES power plant also includes a compressed air storage unit. This leads to time-independent air compression and generation of electrical energy. In charging mode, electrical energy is used to compress air which is stored in underground salt caverns. In discharging mode, the compressed air is reheated using the combustion natural gas and then expanded

to ambient pressure while electrical energy is fed into the grid. The synchronous machine can work as a motor or as a generator by decoupling it from either the turbine or the compressor [20].

Only two CAES power plants have been commissioned worldwide so far: in Huntorf (Germany) and McIntosh (USA) [13]. The plant in Huntorf was commissioned in 1978 and has two turbine stages and a nominal power of 321 MW in discharging mode [21]. The combined volume of the two compressed air salt caverns is $310\,000\,m^3$. The salt caverns operate in a pressure range of 43 to 70 bar [13]. A derivative of the Huntorf power plant is the CAES power plant in McIntosh, which went into operation in 1991. The biggest difference is the exhaust gas recuperation, which uses waste heat from the exhaust gas downstream of the low-pressure turbine to preheat the compressed air upstream of the high-pressure combustion chamber. The CAES power plant at McIntosh has three compressor stages and four turbine stages. At $538\,000\,m^3$, the salt cavern is significantly larger than in Huntorf, but the nominal discharging power is only 110 MW [22].

The diabatic CAES has two decisive disadvantage in today's world: Natural gas is the subject of political disputes and the use of it results in direct greenhouse gas emissions. An alternative is the principle of the adiabatic compressed air energy storage (ACAES) power plant. In this storage concept, the heat generated during the compression of the air is stored in a thermal energy storage unit and used to reheat the air during discharging. Consequently, the plant has no fuel demand [13]. Solid materials such as natural stone, ceramics, concrete and cast iron or liquid media such as nitrate salt and mineral oil are particularly suitable as thermal energy storage for ACAES [23]. The requirements for ACAES thermal energy storage are higher than for other applications in terms of thermal and mechanical stress due to high temperatures and pressures and low pressure losses [13].

Another alternative to convert a compressed air storage power plant into a carbon-free mode of operation is to use hydrogen instead of natural gas to reheat the compressed air before expansion. This concept is called hydrogen compressed air energy storage (HCAES). Figure 1 shows the process flow chart of a proposed retrofit of the Huntorf CAES plant where part of the natural gas is replaced by hydrogen [24]. The addition of a water electrolysis system and a hydrogen storage results in additional storage flexibility.

There are various ways to supply hydrogen. However, only the principle of water electrolysis is suitable for the emission-free and renewable supply of hydrogen. In this process, water (H_2O) is broken down into hydrogen (H_2) and oxygen (O_2) with the help of an electric current. There are three main water electrolysis technologies: Alkaline electrolysis (AEL), polymer electrolyte electrolysis (PEM) and high-temperature water-steam electrolysis (HTE) [25]. High-temperature electrolyzers are not commercially available yet and will therefore not be included in further analysis.

The storage of hydrogen without the use of compressed air can be classified under the term *power-to-gas-to-power*. In a so-called hydrogen energy storage
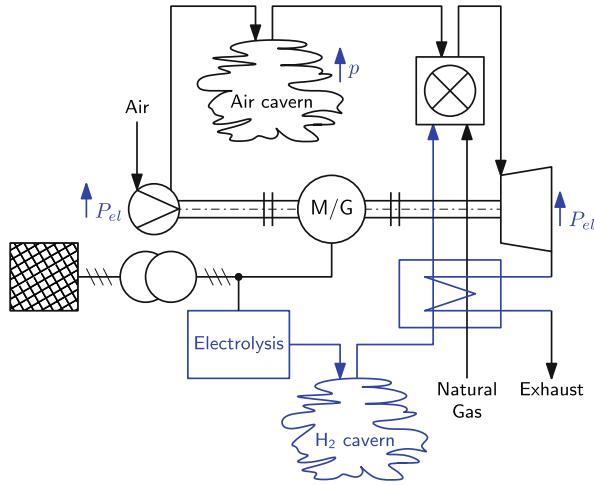
Fig. 1. Process flow chart of a proposed retrofit of the Huntorf CAES plant with a partial replacement of natural gas with hydrogen and the addition of an electrolysis system, a hydrogen storage cavern and recuperation [24].

(HES) power plant, electrical energy is converted into chemical energy in the form of hydrogen, stored in gaseous form and later reconverted into electrical energy. Gas turbine power plants, gas and steam power plants, combined heat and power plants and fuel cells are suitable for reconversion to electricity. Existing gas-fired power plants can in principle be converted to burn hydrogen and, when combined with hydrogen production and storage, can be further developed into a HES power plant [26].

A (hydrogen) gas turbine power plant is very flexible, as the electrical output can be varied between 0 and 100% of nominal power and the start-up time is about 10 min [27]. Because of this flexibility, a gas turbine is to be preferred to a gas and steam power plant or a combined heat and power plant for energy storage plants. The combustion of hydrogen for heating compressed air poses some challenges compared to the use of natural gas. The required mass flow is reduced by 66%, whereby the volume flow is approximately three times greater due to the lower density of hydrogen [28]. The flame speed of hydrogen, on the other hand, is over four times higher than that of methane. The design of the combustion chamber must be adapted so that the flame can be prevented from propagating into the premixing zone [29]. Higher flame temperatures also lead to increased NOx formation, which in turn leads to higher cooling requirements [28].

The *cold combustion* of hydrogen with fuel cells is also suitable for the reconversion into electricity. Within a hydrogen fuel cell, hydrogen (H_2) and oxygen (O_2) react and form water (H_2O). However, hydrogen from salt caverns requires cleaning before it can be used in any fuel cell due to the purity requirements [30].

Table 2 shows an overview of the five large-scale energy storage power plant concepts that will be investigated within this paper based on storing a gaseous

Table 2. Overview of investigated large-scale energy storage power plant concepts.

Abbr.	Description	Storage medium	Reconversion	Figure
CAES	Compressed air energy storage	Compressed air	Natural gas turbine	Fig. 7
ACAES	Adiabatic compressed air energy storage	Compressed air and heat	Expansion turbine	Fig. 8
HCAES	Hydrogen compressed air energy storage	Compressed air and hydrogen	Hydrogen gas turbine	Fig. 9
HES-GT	Hydrogen energy storage	Hydrogen	Hydrogen gas turbine	Fig. 10
HES-FC	Hydrogen energy storage	Hydrogen	Fuel cell	Fig. 11

medium in underground salt caverns. The traditional diabatic CAES presents the disadvantage of a natural gas demand. The logical improvements are the ACAES, where the compression heat is stored, and the HCAES, where the natural gas is replaced by hydrogen. The HES concept is a simplification of the HCAES concept, where hydrogen is reconverted into energy using either an open gas turbine cycle or a fuel cell instead of a compressed air power plant.

In all concepts, hydrogen is produced with water electrolysis and compressed air and hydrogen are both stored in underground salt caverns, while heat is stored in an overground thermal energy storage. Corresponding block diagrams are provided in the appendix. Salt caverns are well suited for the storage of large quantities of compressed air or hydrogen, as they have a high degree of impermeability even when operating on hydrogen, as well as high storage capacities and negligible storage losses. Salt caverns are artificially created cavities in the subsurface that are created with the process of solution mining. Until now, they are mainly used for the storage of liquid and gaseous hydrocarbons [31].

3   Input Data

3.1   Thermodynamic Parameters

Table 3 in the appendix gives an overview of the input data that was used or derived from different references. Some of these parameters will be explained in detail in this section.

Salt Cavern: The geometric volume of a salt cavern describes the size of the cavity. Typical geometric volumes of eligible salt caverns in Europe range from $100\,000\,\text{m}^3$ to $1\,000\,000\,\text{m}^3$ and depend on the geological situation [32]. Depending on the cavern depth and the type of gas that is stored, maximum operating pressures between 60 and 180 bar can be realized [33]. Within this research, a volume of $500\,000\,\text{m}^3$ and a pressure range of 40 to 100 bar is assumed for all salt caverns storing either air or hydrogen.

Electrolysis: Most commercial alkaline electrolysis systems (AEL) are operated at a standard pressure of 10 to 30 bar, while polymer electrolysis systems (PEM) can be operated at 20 to 50 bar. Cell temperatures range between 60 to $90\,^{\circ}\text{C}$ (AEL) and 50 to $80\,^{\circ}\text{C}$ (PEM) [25]. Technology-independent average parameters of 30 bar and $70\,^{\circ}\text{C}$ are assumed for further calculations.

Table 3. Input data.

Symbol	Value	Description	Ref.
V_{SC}	$500\,000\,\mathrm{m}^3$	Geometric volume of the cavern	[32]
p_{min}	40 bar	Minimum operating pressure of the cavern	[77]
p_{max}	100 bar	Maximum operating pressure of the cavern	[77]
η_C, η_T	0.85	Isentropic efficiency of compressor and turbine	[17]
η_{CC}	0.995	Efficiency of the combustion chamber	[44]
η_G	0.985	Efficiency of the synchronous machine	[78]
ϵ_{TS}	0.9	Effectiveness of the heat exchanger (ACAES)	[79]
η_E	0.65	Efficiency of the electrolysis system (HCAES, HES)	Fig. 2
p_E	30 bar	Operating pressure of the electrolysis system (HCAES, HES)	Sect. 3.1
T_E	70 °C	Operating temperature of the electrolysis system (HCAES, HES)	Sect. 3.1
η_{FC}	0.5	Efficiency of the fuel cell system (HES-FC)	Sect. 3
p_{out}/p_{in}	0.95	Pressure loss in combustion chamber (CAES, HCAES, HES-GT)	[45]
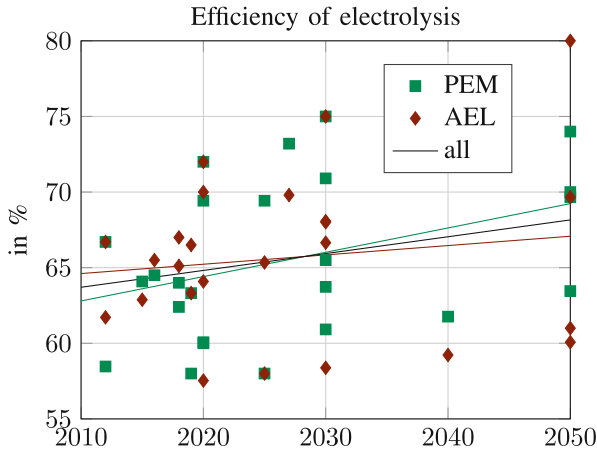
Fig. 2. Efficiency of PEM and AEL electrolysis system dependent on future development based on [12,25,34–41] and [42].

An important parameter is the efficiency of electrolysis, which is given in $\mathrm{MWh_{th}}/\mathrm{MWh_{el}}$ based on the lower heating value. A literature review of electrolysis efficiencies for different technologies incl. peripheral components is shown in Fig. 2. The trend lines are based on a first-degree polynomial. For 2022, the mean value across both technologies is 65.04%. This value includes losses by the secondary components such as pumps and the rectifier.

Fuel Cell: The efficiency of fuel cells is given in $\mathrm{MWh_{el}}/\mathrm{MWh_{th}}$ and includes the secondary components. Literature values range between 50% (today) and 60% (future potential) according to [42]. Staffell et al. [30] give electrical efficiencies between 35 and 60% depending on the technology. According to [43], efficiencies range between 30% and 65% for different technologies. For the following research, an efficiency of 50% is assumed.

3.2   Specific Investment Costs

For estimating the costs of the components of a gas turbine power plant (compressor, combustion chamber, turbine, heat exchanger and generator), the following equations are used based on [44] and [45].

$$C_C = 39.5\,\$/(\text{kg/s}) \cdot \frac{\dot{m}_A}{0.9 - \eta_C} \cdot \beta_C \cdot \ln(\beta_C) \tag{1}$$

$$C_{CC} = 25.65\,\$/(\text{kg/s}) \cdot \frac{\dot{m}_A}{0.995 - p_{out}/p_{ein}}$$
$$\cdot \left(1 + e^{0.018\frac{1}{K} \cdot T_{out} - 26.4}\right) \tag{2}$$

$$C_T = 266.3\,\$/(\text{kg/s}) \cdot \frac{\dot{m}_A}{0.92 - \eta_T} \cdot \ln(\beta_T)$$
$$\cdot \left(1 + e^{0.036\frac{1}{K} \cdot T_{ein} - 54.4}\right) \tag{3}$$

$$C_{HE} = 2290\,\$ \cdot (A_{HE})^{0.6} \tag{4}$$

$$C_G = 26.18\,\$ \cdot (P_G)^{0.95} \qquad \text{with } P_G \text{ in kW}_\text{el} \tag{5}$$

The costs are converted to € using the average exchange rate of 2021 of $1\,€ = 1.18\,\$$. The corresponding operating data are extracted from the thermodynamic calculations. β_i is the pressure ratio and η_i is the isentropic efficiency.

Hydrogen Compressor: Equation 1 describes the costs of an air compressor related to the mass flow of air. Since the material properties and compressor technologies differ significantly for air and hydrogen, Eq. 1 cannot be used for the single-stage compression of hydrogen. Instead, specific costs of $2491\,\$/\text{kW}_\text{el}$ are used to estimate the costs of hydrogen compressors [46].

Heat Exchanger: The CAES and HCAES concepts each have a two-stage compression system with a heat exchanger after every compressor. The HCAES and the two HES concepts have one heat exchanger at the outlet of the hydrogen compressor. The costs for the heat exchangers in the compressor path are added to the compressor costs. CAES and HCAES also have a recuperator that preheats the compressed air from the cavern before it enters the HP combustion chamber. The cost of the recuperator is also determined using Eq. 4 and added to the cost of the turbine. The area of the heat exchangers A_{HE} is calculated based on the amount of heat to be exchanged, the charging and discharging duration, ideal heat exchange condition and a heat exchange coefficient of $50\,\text{W}/(\text{m}^2\,\text{K})$ [47].

Salt Cavern: The investment costs of salt caverns fall exponentially with increasing geometric volume due to economies of scale regarding the solution mining process. As a guideline value, Stolzenburg et al. [36] name $60\,€/\text{m}^3$ for a cavern with $500\,000\,\text{m}^3$ if no infrastructure is yet available on site. In [33], it is stated that the investment costs range between $40\,€/\text{m}^3$ and $100\,€/\text{m}^3$ depending on the infrastructure and geological data situation. [48] quotes $72.32\,€/\text{m}^3$ for a $400\,000\,\text{m}^3$ cavern including costs for the soil survey, the construction and the pipelines for water and brine. If two caverns are built, the costs for the second

cavern are half of the costs for the first cavern, as the solution mining facilities can be used for both caverns [36]. Within this research, a value of $75 €/m^3$ is assumed for one cavern and $56.25 €/m^3$ per cavern for the HCAES concept with two caverns.

Thermal Energy Storage: According to [49], the costs for a solid thermal energy storage are 15 to $40 €/kWh_{th}$ and for a liquid thermal energy storage 20 to $50 €/kWh_{th}$. Rundel et al. [50] specify investment costs of 30 to $40 €/kWh_{th}$ (liquid salt medium) or 15 to $20 €/kWh_{th}$ (solid medium). In the following, $25 €/kWh_{th}$ is assumed.

Electrolysis: In order to estimate the investment costs of electrolysis systems, an extensive literature review was carried out. The results for PEM and AEL electrolysis systems including peripheral components are shown in Fig. 3. In addition, a trend line in the form of an exponential function was calculated for each technology and across both technologies. For 2022, an average technology-independent price of $1074 €/kW$ based on the trend line is used for further calculations.

Fuel Cell: Niakolas et al. [54] give costs of 4500 to 8000 €/kW for a stationary fuel cell. The International Energy Agency gives investment costs between 3000 and 5000 $/kW in a 2015 publication [55] and 1600 $/kW in a 2019 publication [42]. Maleki et al. [56] state 6667 $/kW and in [57], 5000 $/kW are given. In [58], specific investment costs of 4000 to 5000 €/kW are given for system with more than 400 kW. In the following, specific investment costs of 2500 €/kW are assumed. This value already includes the costs for peripheral equipment.
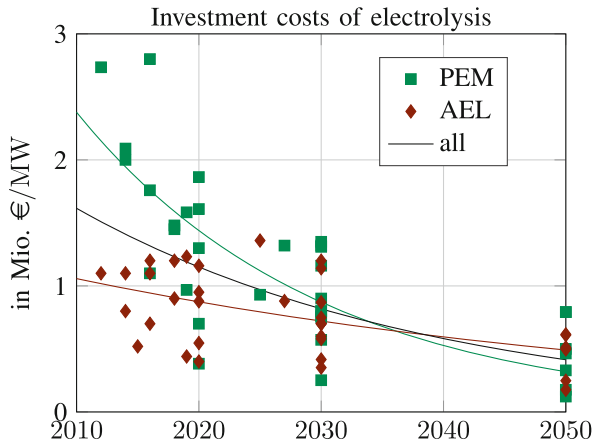
Fig. 3. Development of investment costs for electrolysers of different technologies with exponential trend line per electrolysis technology and technology-independent trend line in black. Based on [12,25,34–40,42,51,52] and [53].

4   Criteria for Comparison

4.1   Storage Capacity and Round-Trip Efficiency

Thermodynamic analyses of the concepts are based on the first and second law of thermodynamics. The methodology is based on Safaei et al. [17]. One complete charging and discharging cycle at full load is considered (no part-load operation). The goal is to calculate the storage capacity in charging mode and the round-trip efficiency based on a simplified process analysis. Block diagrams, detailed formulae and input parameters are presented in the appendix. The following assumptions are made:

- ideal gas conditions
- isentropic and adiabatic compression and expansion, isobaric heat exchange, adiabatic storage
- variable compression and expansion rate according to the instantaneous cavern pressure
- steady state conditions in the caverns at the beginning of each compression and expansion process
- negligible mass of fuel in comparison to mass of air at the turbine inlet
- constant efficiencies at nominal operating point

The electrical storage capacity equals the amount of work needed for one full charging cycle and is mainly determined by the size of the caverns, which is predefined with $500\,000\,\mathrm{m}^3$ (Sect. 3.1). Figure 4 shows the results of the thermodynamic calculations. With 3.9 GWh, the CAES has the lowest storage capacity equal to the consumed energy in charging mode. The storage capacity of the ACAES is slightly higher than that of the CAES, even though both concepts use the same amount of air and the same pressure difference in the cavern. But the outlet temperature of the ACAES compressors is higher in order to be able to store more heat in the thermal energy storage. This increases the inlet temperature and thus the energy demand of the high pressure compressor.

The HCAES concept includes two salt caverns: one for storing compressed air and one for hydrogen. Only a fraction of the hydrogen storage is needed to fully discharge the compressed air storage. The storage capacity of 14.5 GWh of the HCAES in charging mode is composed of the work to compress air for one full charging cycle of the air storage and the work to produce and compress as much hydrogen as is needed for one discharging cycle of the air storage. If the storage capacity of the HCAES is related to the possibility of storing surplus energy, the storage capacity of the entire hydrogen storage must be added to the capacity of the compressed air storage. This leads to a storage capacity of 85.7 GWh, which is slightly higher than for the HES concepts. At 81.8 GWh, the storage capacity of both HES concepts equals the amount of electricity needed to produce and compress hydrogen to be stored at 100 bar in a $500\,000\,\mathrm{m}^3$ salt cavern.

Because of the electrolysis operating pressure of 30 bar, the subsequent compression of hydrogen requires only little energy compared to the energy demand
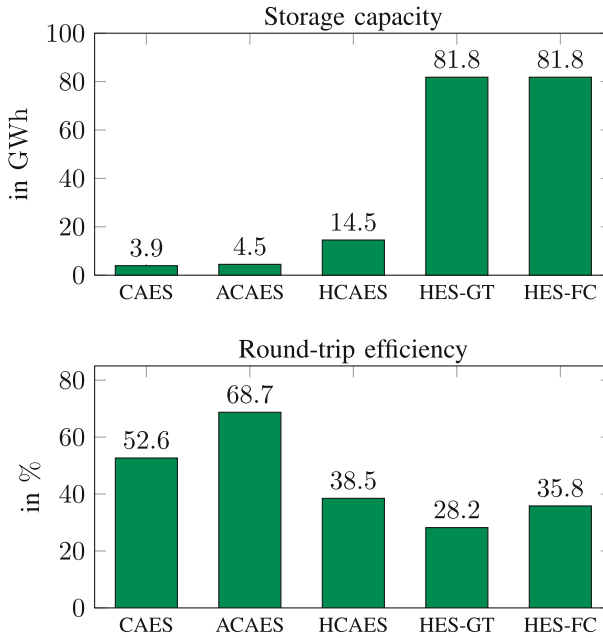
Fig. 4. Charging storage capacity and round-trip efficiency based on thermodynamic calculations and uniform input parameters.

of the electrolysis itself. In the HCAES, the consumed energy in charging mode is composed of the work of the air compressor (27%), the electrolysis (72.3%) and the hydrogen compressor (0.7,%). In the HES concept, 99.2% of the work in charging mode is used for the electrolysis and 0.8% for the subsequent compression of the hydrogen.

The round-trip efficiency is defined as the quotient of the discharged energy divided by the charged energy during one full charging and discharging cycle. For all concepts except the CAES, this corresponds to the consumed and generated electrical energy respectively. The CAES has an additional fuel demand, which is added to the electrical energy demand in the denominator (Eq. 22). The fuel demand accounts for 63.1% of the total energy demand of the CAES.

The round-trip efficiency of the conventional CAES is 52.6%. For ACAES, the round-trip efficiency increases to 68.7% because most of the heat that accumulates when compressing air is stored and used during discharging mode. On the other hand, if the compressed air storage power plant is operated with hydrogen (HCAES), the round-trip efficiency decreases to 38.5% because of the additional work required to produce and compress hydrogen. Using compressed air in the hydrogen combustion chamber increases the fuel efficiency, which is why the round-trip efficiency of HCAES is higher than of the HES-GT. The same correlation can be seen in [59] when comparing CAES to an open gas turbine cycle. The round-trip efficiency of the HES-FC concept is slightly higher than

the round-trip efficiency of the HES-GT concept because the fuel cell in the reconversion path has a higher efficiency than the gas turbine.

To discuss the results, values are compared to suitable literature. The existing CAES plant in McIntosh (USA) has, in contrast to the plant in Huntorf, a recuperator and a round-trip efficiency of 54% [13], which confirms the calculated value of 52.6%. Schmidt et al. [8] specify a round-trip efficiency of 44% without detailing the CAES concept. For ACAES round-trip efficiencies, values of 68.8% [4], 71%% [6], 70 to 89% [9], 63% [10] and 70% [13] are given in the literature. The calculated value of 68.7% lies on the lower end of that range.

Hydrogen energy storage (HES) efficiencies of 39.9% [4], 42% [6] and 40% [8] are given in the literature without specifying the reconversion path. The round-trip efficiency of HES-GT is given with 43% in [10] and 24% in [11]. The efficiency in [10] is a little higher because they assume an electrolysis efficiency of 73%. HES-FC efficiencies are given with 30 to 42% in [9] and 48% in [10] (higher electrolysis efficiency).

Comparing the results to the round-trip efficiency of pumped hydro storage (PHS) and lithium-ion battery storage systems (Li-Ion), it becomes apparent that both technologies possess higher efficiencies than cavern-based storage concepts. For PHS, values of 79.2% [4], 85% [6], 65% [7], 78% [8] and 70 to 82% [9] are stated in the literature. Lithium-Ion batteries have even greater efficiencies of e.g. 85 to 95% [7], 86% [8], 85 to 95% [9] and 93.5% [11].

4.2   Technology Readiness Level

The technology readiness level (TRL) is used to compare the maturity of different types of technology. A TRL of 1 implies the lowest maturity where only basic principles were observed thus far. A TRL of 9 describes the highest maturity and entails that the actual system is proven in an operational environment and that competitive manufacturing of key technologies is available [60].

CAES shows the best commercial viability since it is the only concept which has been commissioned so far. It is assigned a TRL of 8, meaning the system is complete and qualified for operation, due to the fact that only two plants worldwide are in operation [61].

As for ACAES, the thermal energy storage restricts its commercial viability. High temperatures are needed to keep the number of compressor and turbine stages low. Ideally, the thermal storage must operate adiabatically and isobarically and have a good partial load efficiency with regard to lower air mass flows. As a result, such thermal storage must have a significantly larger heat transfer surface than conventional heat exchangers [18]. Additionally, compressors for ACAES are different than conventional air compressors because the objective is to recover as much heat as possible to store and use during discharging mode. Conventional compressors are designed to dissipate as much heat as possible during the compression process. The TRL of ACAES is therefore rated with 4 (the technology is validated in a lab) according to [61].

The TRL of electrolysis depends heavily on the technology and the rated power. Pinsky et al. [62] assume a TRL of 9 for alkaline electrolysis and 6–8 for

PEM. The largest operating electrolysis with 20 MW is the Air Liquide Becancour Project in Canada according to the IAE [63]. Over 200 projects worldwide with electrolysis systems in the MW and GW range have been announced for the coming 15 years [63]. Independent on the type of electrolysis, the TRL of an electrolysis system in the 100 MW range is set at 7, meaning a system prototype in an operational environment was demonstrated.

The storage of hydrogen in underground salt caverns requires only minor research and development efforts because of the long experience with storing natural gas. Research questions concern mainly the cement integrity and specifications for the utilized overground equipment. So far, several salt caverns in the UK and the US have been operated with hydrogen for up to 40 years [33]. Because no hydrogen salt cavern has been put into operation recently, a TRL of 8 is assigned.

Large-scale hydrogen gas turbines are not yet commercially available, even though technological modifications would only be moderate [55]. The IEA rates the maturity of hydrogen gas turbines with "pre-commercial demonstration" [64]. As one of the leading gas turbine providers, Siemens Energy states that they have one medium-scale gas turbine model with up to 38 MW that can be operated with pure hydrogen and a large-scale gas turbine that runs on up to 60% hydrogen [26]. A gas turbine by GE with 11.4 MW has been operated with 97.5% hydrogen since 2010 [29]. The TRL of hydrogen gas turbines is consequently rated with 7 (system prototype demonstration in operational environment).

Commercially available fuel cells present to date rated powers of up to 11 MW according to [65]. There is however still research and prototyping needed to increase the maturity of multi-MW fuel cells with regard to robustness and manufacturability [65]. The IEA assumes a maturity of high-temperature fuel cells between "pre-commercial demonstration" and "commercial operation in relevant environment" [64]. In conclusion, the TRL of large-scale hydrogen fuel cells is assumed at 6, meaning the technology has been demonstrated in a relevant environment.

The technology readiness level of each storage plant concept equals the minimum TRL of any component, as it is the limiting factor [62]. Therefore, the TRL of CAES is 8, while HCAES and HES-GT present a TRL of 7. The TRL of HES-FC is 6 and the ACAES concept has the lowest TRL with 4 due to the thermal energy storage.

4.3   Investment Costs

In the following, the power-related and capacity-related investment costs of the storage power plant concepts are estimated. Costs for project planning, land use, site development, access roads and grid connection are not taken into account.

The costs scale with the nominal power of the components. For comparability, charging and discharging nominal electrical power are therefore set equal for all concepts. As these concepts are predefined as long-term storage power plants, the discharging duration is set to be at least 24 h [3, Chap. 2]. The ACAES has the lowest discharging capacity and thus determines the nominal power of 128.3 MW.

This results in charging durations of more than 600 h for the HES concepts for one full charging cycle due to the high storage capacity of the hydrogen storage cavern. The nominal power in both charging and discharging mode and the resulting charging and discharging durations of the concepts are shown in Table 4 in the appendix. The nominal power in charging mode is divided between compressed air and, if applicable, electrolysis and hydrogen compression scaling with the energy demand. The investment costs of each concept are based on the nominal electrical power and the specific investment costs (Sect. 3.2). Table 5 in the appendix shows the resulting total investment costs for each component for the five storage power plant concepts.

Figure 5 shows the specific investment costs of the concepts related to the nominal power and the storage capacity in charging mode. With 402 €/MW, the power-related specific investment costs of the CAES are the lowest. In contrast, the power-related specific investment costs of the HES-FC are ten times higher with the fuel cell being the most expensive component, accounting for 64% of the total costs. Despite the costs for the second cavern, the HCAES is less expensive than the HES-GT because the electrolysis is smaller. The ACAES concept has the highest capacity-related investment costs. This is mainly due to the thermal energy storage, which accounts for 63% of the total costs. The capacity-related investment costs of the HES-GT are the lowest.

Table 4. Nominal electrical power (equal in charging and discharging mode) and charging and discharging duration of each energy storage concept.

Concept	Nominal power	Charging duration	Discharging duration
CAES	128.3 MW	30.6 h	43.6 h
ACAES	128.3 MW	34.9 h	24 h[a]
HCAES	128.3 MW	113.3 h	43.6 h
HES-GT	128.3 MW	637.6 h	179.8 h
HES-FC	128.3 MW	637.6 h	228.4 h

[a]Reference parameter.

Table 5. Component investment costs and total investment costs for each energy storage concept.

Component	CAES	ACAES	HCAES	HES-GT	HES-FC
Air compressor	9.23 Mio €	5.73 Mio €	3.25 Mio €	-	-
Electrolysis	-	-	99.70 Mio €	136.67 Mio €	136.67 Mio €
Hydrogen compressor	-	-	3.05 Mio €	3.67 Mio €	3.67 Mio €
Compressed air storage	37.50 Mio €	37.50 Mio €	28.13 Mio €	-	-
Hydrogen storage	-	-	28.13 Mio €	37.50 Mio €	37.50 Mio €
Heat storage	-	83.43 Mio €	-	-	-
Turbine	3.25 Mio €	4.48 Mio €	2.91 Mio €	10.21 Mio €	-
Fuel cell	-	-	-	-	320.83 Mio €
Motor/Generator	1.58 Mio €	1.58 Mio €	1.58 Mio €	1.58 Mio €	0.02 Mio €
Sum	51.63 Mio €	132.73 Mio €	166.74 Mio €	189.63 Mio €	498.69 Mio €
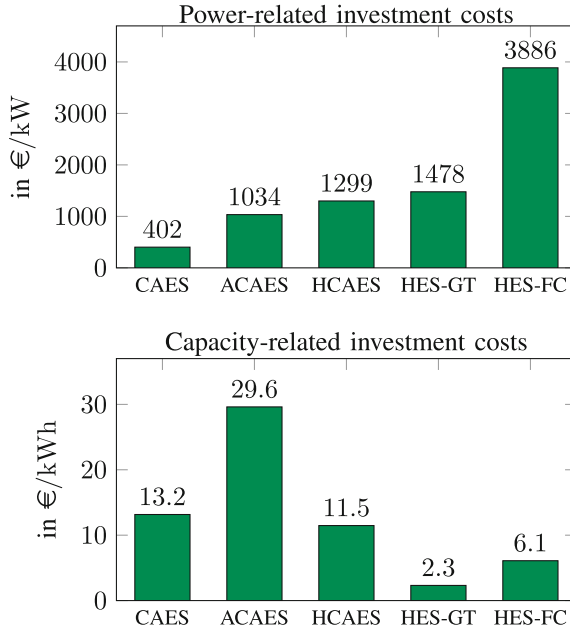
Fig. 5. Specific investment costs of the storage power plant concepts related to the nominal power and the storage capacity in charging mode.

To contextualize the results, it is attempted to compare the calculations to suitable literature. [8] give investment costs for conventional CAES of 871 $/kW, while [14] state a range from 400 to 1000 €/kW. Capacity related investment costs are specified with 39 $/kW [8] and 2 to 120 €/kWh [14].

Literature values for power-related investment costs for ACAES include 910 €/kW [4] and 893 €/kW [9] and for capacity-related investment costs 21 €/kWh [4], 46 $/kWh [6] and 92 €/kWh [9].

Power-related investment costs of HES are given with 2500 €/kW in [4], 5417 $/kW in [8] and 1570 €/kW (HES-GT) resp. 3243 €/kW (HES-FC) in [9]. Capacity-related investment costs vary widely between 0.3 €/kWh [4], 151$/kWh [6], 31 $/kWh [8] and 262 €/kWh (HES-GT) resp. 540 €/kWh (HES-FC) [9] in corresponding literature.

The values of the cavern-based storage concepts can be compared to pumped hydro storage (PHS) and lithium-ion (Li-Ion) batteries to evaluate the results. Power-specific investment costs of pumped hydro storage (PHS) are with e.g. 487 €/kWh [4], 1129 $/kW [8] and 1406 €/kW [9] in the same range of costs for all three CAES concepts and HES-GT. Capacity-related investment costs of PHS (e.g. 57 €/kWh [4], 97 $/kWh [6], 80 $/kWh [8] and 137 €/kWh [9]) are considerably higher than the costs of every cavern-based storage concept. Li-Ion batteries have average power-related investment costs (e.g. 678 $/kW [8],

1160 €/kW [9]), but substantially higher capacity-related investment costs (e.g. 802 $/kWh [8], 546 €/kWh [9]).

4.4   Additional Non-countable Criteria for Comparison

Additional criteria, that will be compared based on qualitative correlations, include ability to provide of ancillary services, storage losses, greenhouse gas emissions and demand for land. In order to be able to compare the storage power plant concepts on the basis of all quantitative and qualitative criteria, a ranking is established for each criterion. For the quantitative criteria, this is done using the numerical values of the calculated parameters (e.g. the concept with the highest round-trip efficiency is ranked first and the concept with the lowest round-trip efficiency is ranked fifth). The ranking of qualitative criteria is done using comparison of pairs. This method allows the systematic comparison of non-countable criteria by comparing each concept pairwise to another concept with regard to one criterion. If concept A is better than concept B, A receives two points while B receives zero points. If both are equal, both concepts receive one point. Ranks are established based on the sum of points of each concept.

Ancillary Services: The demand and supply of power in a power grid needs to be balanced at every instance to ensure proper operation. Unforeseen deviations of the demand or the supply have to be managed by making use of the flexibility of the grid participants. These so-called ancillary services are frequency control, voltage control, system control and system restoration [66]. The frequency control includes instantaneous reserve, primary balancing reserve, secondary balancing reserve and minute reserve. All but the instantaneous reserve are managed within their own reserve market.

The dynamic simulation of different storage concepts providing ancillary service can be witnessed in corresponding literature and is not within the scope of this research. Calero et al. [67] developed a dynamic model of a CAES with a detailed submodel for the synchronous machine and showed that a CAES is well suited to provide primary frequency control. The dynamic behavior of a hybrid storage system consisting of ACAES and flywheel energy storage is analyzed in [68]. Within this approach, the ACAES is used to compensate fluctuating wind power generation with low frequency and high amplitude ($f \leq 0.5\,\mathrm{Hz}$).

Within this research, the provision of instantaneous reserve by the power unit of the storage power plant is considered. The power unit is either a synchronous machine, an inverter or a rectifier, depending on the storage concept. Historically, instantaneous reserve has been mostly provided by generators of fossil power plants. For 2030, roughly two thirds of the demand for instantaneous reserve have to be provided by alternative sources [66]. According to [69], a CAES or ACAES plant can provide instantaneous reserve in charging and discharging mode with its synchronous machine, whereas a HES-GT can only provide it in discharging mode. Power electronics, such as the rectifier of the electrolysis system and the inverter of the fuel cell, can emulate the behavior of a synchronous machine and therefore provide instantaneous reserve with a

suitable control system. However, the system either needs additional short term energy storage or has to be operated below the rated power for supplying energy for the virtual inertia. Suitable short term energy storage technologies are e.g. supercapacitors and flywheels [70].

The provision of instantaneous reserve is ranked best for CAES, ACAES and HCAES because all concepts use a synchronous machine in both charging and discharging mode. The HES-GT uses a synchronous motor in charging mode only for the compression of hydrogen with little power demand, but the concept possesses a synchronous generator for the gas turbine in discharging mode. The HES-FC is ranked worst because it includes only a small motor for hydrogen compression and a rectifier and an inverter which have to be modified to provide instantaneous reserve.

Greenhouse Gas Emissions: The diabatic compressed air storage power plant is the only concept that has direct carbon emissions due to the use of natural gas. When hydrogen is burned in the HCAES and HES-GT concepts, however, the high flame temperatures lead to increased amounts of nitrogen oxide, which has noxious effects. The combustion of pure hydrogen produces almost four times as much NOx as the combustion of methane [28]. This results in the shared first rank for ACAES and HES-FC (no emissions), the shared third rank for HCAES and HES-GT (no carbon emissions) and the last rank for CAES.

Storage Losses: Salt caverns are technically tight due to good creep properties of the salt rock, as long as the maximum operating pressure is maintained [32]. The losses of a thermal energy storage are 2 to 4% of the storage capacity per day [49]. This results in the divided first rank for every storage concept except ACAES (rank 5).

Demand for Land: The CAES shows the lowest demand for land, since the only overground facilities are the compressors, combustion chambers, turbines and recuperation. Because of the electrolysis, the demand for land of HCAES and HES-GT is slightly higher. The fuel cell of the HES-FC increases the demand for land additionally. The ACAES has the highest demand for land because of the thermal energy storage [18].

5   Results of Comparison

The results of the comparison of the five storage concepts based on quantitative and qualitative criteria are shown in Fig. 6. The axis represents the rank of each concept, with $x = 1$ being the best rank and $x = 5$ being the worst rank. A smaller outline represents a better overall performance.

If all criteria are weighted equally, the HCAES concept shows the best average rank with 2.0, followed by the CAES with 2.1. The HES-GT concept has an average rank of 2.3, while HES-FC and ACAES have average ranks of 3 and 3.2 respectively. However, depending on the situation, not all criteria should be weighted equally.
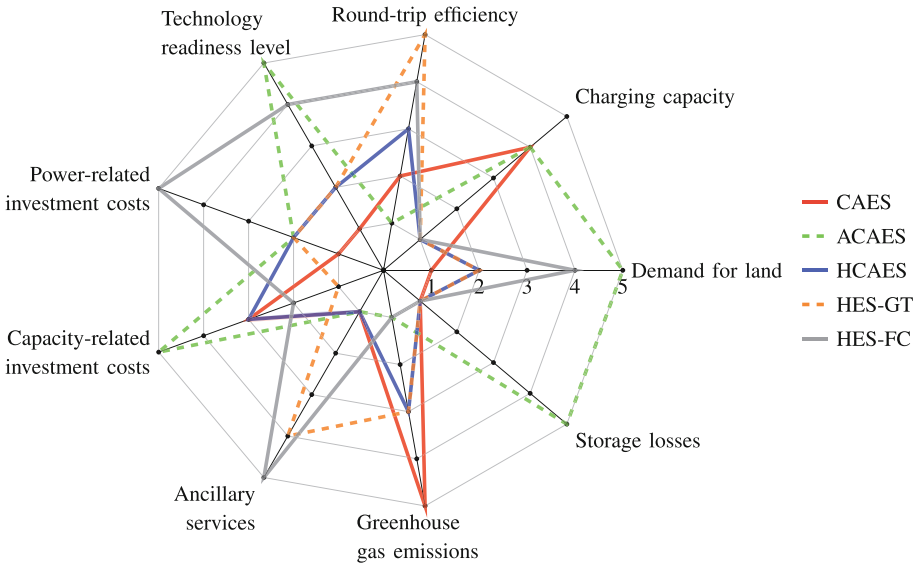
Fig. 6. Comparison of the storage power plant concepts based on quantitative and qualitative criteria by means of a ranking based on a pairwise comparison ($x = 1$ being the best rank and $x = 5$ being the worst rank).

Within a renewable energy system, the CAES cannot be used because of its direct carbon dioxide emissions, which can be considered as a knock-out criterion with regard to climate change restrictions. ACAES should not be used for long-term storage of electrical energy because of high storage losses between operation. The low round-trip efficiency of HES-GT becomes less relevant in an energy system with a high amount of excess renewable energy. If the goal is to store as much excess renewable energy as possible, the HES-GT and the HES-FC are most suitable because of high charging capacities and low capacity-related investment costs. On the other side, HES-FC is not suitable for peak shaving due to high power-related investment costs. The high demand for land of both ACAES and HES-FC becomes less significant if the land is abundant or can be used additionally by installing a solar system on the rooftop of the overground facilities. For energy storage solutions that can be installed in the short-term future, HCAES and HES-GT are most suitable due to high technology readiness levels. With further development of thermal energy storage and large-scale stationary fuel cells, both ACAES and HES-FC become more viable.

6   Discussion

The thermodynamic analysis of the concepts is a simplified representation of the reality. A more detailed analysis goes beyond the scope of this paper. Further analysis should include part-load efficiencies of the compressor and the turbine

dependent on the instantaneous pressure ratio due to the pressure change in the cavern, as it is seen in [71]. Zhao et al. [68] formulate dynamic compressor and turbine models using variable isentropic efficiencies and specific heat capacities. Due to the variable output pressure, compressors and turbines also have to operate with variable mass flows to achieve constant power. This presents significant challenges to the design and operation of all compressed air concepts [18]. Additionally, both the compression, the expansion and the storage are assumed to be adiabatic. For a more detailed analysis, the heat exchange with the environment should be considered, as it is done for the storage cavern of an ACAES for example in [72] and [73]. Round-trip efficiencies can also be calculate and compared based on exergy instead of energy, as it is seen for example for a CAES in [59].

Furthermore, the thermodynamic process of each concept can be optimized with further research. For example, most fuel cells are operated at low pressures, often ambient pressure. With an additional expansion turbine between the salt cavern and the fuel cell, the discharging work and thus the efficiency would increase. In the other concepts, an additional expansion turbine at the outlet of the storage cavern can also decrease the operating pressure and thus the costs of turbines and combustion chambers.

Hydrogen components such as electrolyzers and fuel cells are the subject of various research projects and present a high development potential regarding efficiency and investment costs. The efficiency of the electrolysis is expected to rise to 68% by 2050 (Fig. 2). At the same time, fuel cell efficiencies are expected to increase to 60% [74]. This would lead to an increase in round-trip efficiency for HCAES to 41.4%, HES-GT to 31.1% and HES-FC to 44.9%. Further improvement of efficiencies of gas turbine components are not expected.

Additionally, it is expected that electrolysis costs decrease to 414€/kW by 2050 (Fig. 3) while fuel cell costs could decrease by 63% if the production rate increases from 100 to 50000 units per year [75] or by 45% in 2030 compared to 2021 [65]. This would lead to a decrease in total investment costs by 37% (HCAES), 45% (HES-GT) and 56% (HES-FC with 1000€/kW for fuel cells).

As mentioned before, costs for project planning where not taken into account. It is to be suspected that those costs rise with lower technology readiness levels because of the increasing need for system engineering. With a TRL of 8, the CAES is expected to have the lowest project planning costs. With low TRL, HES-FC and ACAES are expected to have significantly higher project planning costs. This would lead to even higher differences in power-related investment costs but more levelized capacity-related investment costs if project planning costs are considered.

7   Conclusion

This paper aims at comparing different concepts for large-scale, long-term energy storage based on storing air or hydrogen in salt caverns. Five concepts are considered: diabatic compressed air energy storage (CAES), adiabatic compressed air energy storage (ACAES), hydrogen compressed air energy storage (HCAES),

hydrogen energy storage with a gas turbine (HES-GT) and hydrogen energy storage with a fuel cell (HES-FC). Uniform input data is defined for the thermodynamic calculation of storage capacity and the round-trip efficiency based on the first and second law of thermodynamics. Specific investment cost equations for gas turbine power plant components are derived from technical correlations. Additionally, specific investment costs of salt cavern, electrolysis, fuel cell and thermal energy storage are derived from an extensive literature review. The concepts are also compared based on the technology readiness level, provision of ancillary services, storage losses, greenhouse gas emissions and demand for land.

The ACAES presents the highest efficiency with 69%, while HES-GT has the lowest efficiency with 28%. The other concepts range between 53% (CAES), 39% (HCAES) and 36% (HES-FC). The storage capacity of CAES and ACAES is less than 5 GWh. The storage capacity of both HES concepts is 20 times higher with over 80 GWh. This results in charging durations of 30 h (CAES) to 630 h (HES) for a nominal electrical power of 130 MW.

Total investment costs for a storage power plant with 130 MW in charging and discharging mode range between 52 Mio € (CAES) and 499 Mio € (HES-FC). The components with the highest investment costs are the electrolysis of HCAES and HES, the thermal energy storage of ACAES and the fuel cell of HES-FC. Air and hydrogen compressors, turbines and the generator are far less expensive in comparison. Specific investment costs related to the nominal power assume values of 402 €/kW (CAES) to 3886 €/kW (HES-FC) and are competitive to costs of pumped hydro storage and lithium-ion batteries. Capacity-related investment costs lie below 30 €/kWh for every concept and are therefore considerably lower than for PHS and Li-Ion.

All concepts have different advantages and disadvantages. The diabatic CAES is the only concept with direct carbon emissions, but it is also the only concepts that has been commissioned so far. To eliminate carbon emissions, the compression heat can be stored and used during expansion or natural gas can be substituted with hydrogen. Existing CAES plants can be transformed into a hydrogen compressed air energy storage plant by substituting natural gas with hydrogen. This approach has been researched recently regarding the Huntorf CAES power plant in Germany [76]. The transformation not only leads to zero carbon emissions, it also greatly improves the operational flexibility of the plant by adding an electrolysis system and a hydrogen cavern [24]. The storage of compressed air leads to better fuel efficiencies of the HCAES compared to a hydrogen gas turbine power plant (HES-GT).

Appendix

Thermodynamic Calculations

The round-trip efficiency and the storage capacity are calculated using simplified thermodynamic correlations based on the first and second law of thermodynamics. The approach is based on and explained in detail in [17].
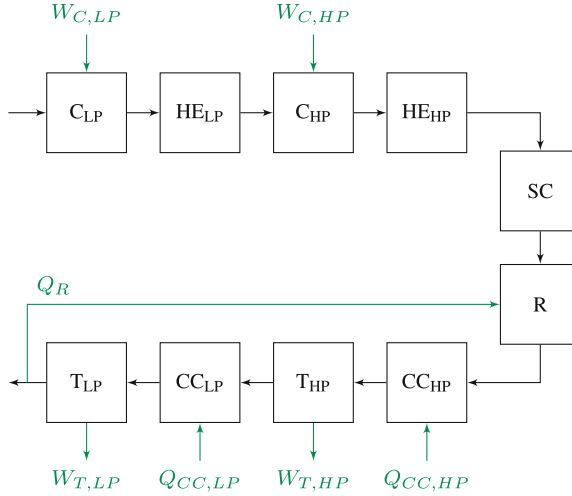
Fig. 7. Block diagram of a compressed air energy storage power plant (CAES), C - compressor, HE - heat exchanger, SC - salt cavern, R - recuperation, CC - combustion chamber, T - turbine, LP - low pressure, HP - high pressure.

CAES: Figure 7 shows the block diagram of the compressed air energy storage concept.

In charging mode, the input temperature of the cavern is predetermined and corresponds to the output temperature of the HP heat exchanger ($T_{SC,in} = T_{HE,HP,out} = 30\,°\text{C}$). It is assumed that the output temperature of the LP heat exchanger, and thus the input temperature of the HP compressor, also corresponds to the input temperature of the cavern ($T_{C,HP,in} = T_{HE,LP,out} = T_{SC,in}$). The LP compressor input temperature equals the ambient temperature. The mass of air stored during charging mode is equal to Eq. 6.

$$m_{A,ch} = \frac{V \cdot (p_{max} - p_{min})}{R \cdot \kappa \cdot T_{SC,in}} \tag{6}$$

The entire work of compressing air during charging mode is comprised of the work of the LP and the HP compressor.

$$W_{C,A} = \int_{p_{min}}^{p_{max}} \mathrm{d}W_{C,A,LP} + \int_{p_{min}}^{p_{max}} \mathrm{d}W_{C,A,HP} \tag{7}$$

$$\mathrm{d}W_{C,A,i} = c_P \cdot (T_{C,i,in} - T_{C,i,out})\,\mathrm{d}m_{A,ch} \tag{8}$$

$$T_{C,i,out} = T_{C,i,in} - \frac{T_{C,i,in} - T_{C,i,out,mom}}{\eta_C} \tag{9}$$

$$T_{C,i,out,mom} = T_{C,i,in} \cdot \left(\sqrt{\frac{p_{SC}}{p_0}} \right)^{\frac{\kappa-1}{\kappa}} \tag{10}$$

$$\mathrm{d}m_{A,ch} = \frac{V}{R \cdot \kappa \cdot T_{SC,in}} \mathrm{d}p_{SC} \tag{11}$$

The work of both turbines in discharging mode is calculated according to Eq. 12. The inlet temperature of the HP turbine is set at $530\,°C$, while the inlet temperature of the LP turbine is $850\,°C$.

$$W_T = \int_{p_{min}}^{p_{max}} \mathrm{d}W_{T,HP} + \int_{p_{min}}^{p_{max}} \mathrm{d}W_{T,LP} \tag{12}$$

$$\mathrm{d}W_{T,i} = c_P \cdot (T_{T,i,in} - T_{T,i,out}) \, \mathrm{d}m_{A,dch} \tag{13}$$

$$T_{T,i,out} = T_{T,i,in} - \eta_T \cdot (T_{T,i,in} - T_{T,i,out,mom}) \tag{14}$$

$$T_{T,i,out,mom} = T_{T,i,in} \cdot \left(\sqrt{\frac{p_0}{p_{SC}}} \right)^{\frac{\kappa-1}{\kappa}} \tag{15}$$

$$\mathrm{d}m_{A,dch} = \frac{V}{R \cdot \kappa \cdot T_{SC}} \mathrm{d}p_{SC} \tag{16}$$

$$T_{SC} = T_{SC,max} \cdot \left(\frac{p_{SC}}{p_{max}} \right)^{\frac{\kappa-1}{\kappa}} \tag{17}$$

The fuel requirement equals the energy demand to heat the air to the turbine inlet temperature (Eq. 18). Before the HP combustion chamber, the air is heated by recuperation with $T_R = 130\,°C$ as the outlet temperature of the exhaust gas (see Eq. 21).

$$Q_{CC} = \int_{p_{min}}^{p_{max}} \mathrm{d}Q_{CC,HP} + \int_{p_{min}}^{p_{max}} \mathrm{d}Q_{CC,LP} \tag{18}$$

$$\begin{aligned} \mathrm{d}Q_{CC,LP} &= c_P \cdot (T_{CC,LP,out} - T_{CC,LP,in}) \, \mathrm{d}m_{A,dch} \\ &= c_P \cdot (T_{T,LP,in} - T_{T,HP,out}) \, \mathrm{d}m_{A,dch} \end{aligned} \tag{19}$$

$$\begin{aligned} \mathrm{d}Q_{CC,HP} &= c_P \cdot (T_{CC,HP,out} - T_{CC,HP,in}) \, \mathrm{d}m_{A,dch} \\ &= c_P \cdot (T_{T,HP,in} - T_{CC,HP,in}) \, \mathrm{d}m_{A,dch} \end{aligned} \tag{20}$$

$$T_{CC,HP,in} = T_{SC} + (T_{T,LP,out} - T_R) \tag{21}$$

The round-trip efficiency of a CAES equals the work of the turbine divided by the sum of the compressor work and the fuel demand.

$$\eta_{CAES} = \frac{W_T}{|W_{C,A}| + Q_{CC}} \tag{22}$$

ACAES: The block diagram of the adiabatic compressed air energy storage concept is shown in Fig. 8.

The calculation of the compressor work in charging mode is analogue to the CAES (Eq. 6 to 11). However, the maximum output temperature of the HP compressor is a predefined parameter of $600\,°C$. Thus, the input temperature $T_{C,HP,in}$ can be calculated with Eq. 9 and 10.

The amount of heat the thermal energy storage i (HP or LP) delivers in discharging mode corresponds to the amount of heat stored in charging mode minus the losses defined by the effectiveness of the thermal energy storage with
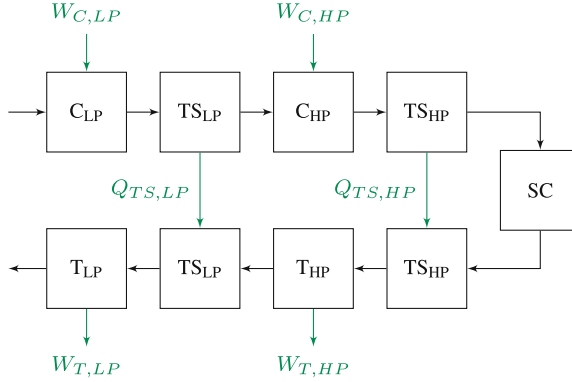
Fig. 8. Block diagram of an adiabatic compressed air energy storage power plant (ACAES), C - compressor, TS - thermal energy storage, SC - salt cavern, T - turbine, LP - low pressure, HP - high pressure.

$T_{TS,HP,dch,in} = T_{SC}$ and $T_{TS,LP,dch,in} = T_{T,HP,out}$.

$$Q_{TS,i,dch} = \int_{p_{min}}^{p_{max}} dQ_{TS,i,dch} = \epsilon_{TS} \cdot Q_{TS,i,ch} \tag{23}$$

$$dQ_{TS,i,dch} = c_p \cdot (T_{TS,i,dch,out} - T_{TS,i,dch,in}) dm_{A,ch} \tag{24}$$

The temperature at the inlet of the HP turbine is equal to the temperature at the outlet of the HP thermal storage ($T_{T,HP,in} = T_{TS,HP,dch,out}$). The calculation of the turbine work in discharging mode is analogue to the CAES (Eq. 12 to 17).

The round-trip efficiency of the ACAES equals the turbine work divided by the compressor work:

$$\eta_{ACAES} = \frac{W_T}{|W_{C,A}|} \tag{25}$$

HCAES: Figure 9 shows the block diagram of the hydrogen compressed air energy storage concept.

The calculations of the consumed work to compress the air in charging mode and the turbine work during discharging mode as well as the fuel demand are analogue to the CAES. The energy demand of the electrolysis is determined using the fuel demand and the efficiency. From the fuel demand and the lower heating value LHV_H, the mass of hydrogen is obtained.

$$W_E = \frac{Q_{CC}}{\eta_E} \tag{26}$$

$$m_{H,ch} = m_{H,dch} = \frac{Q_E}{LHV_H} \tag{27}$$

After electrolysis, the hydrogen is compressed to the pressure of the cavern with a single-stage compression including downstream cooling. The inlet temperature
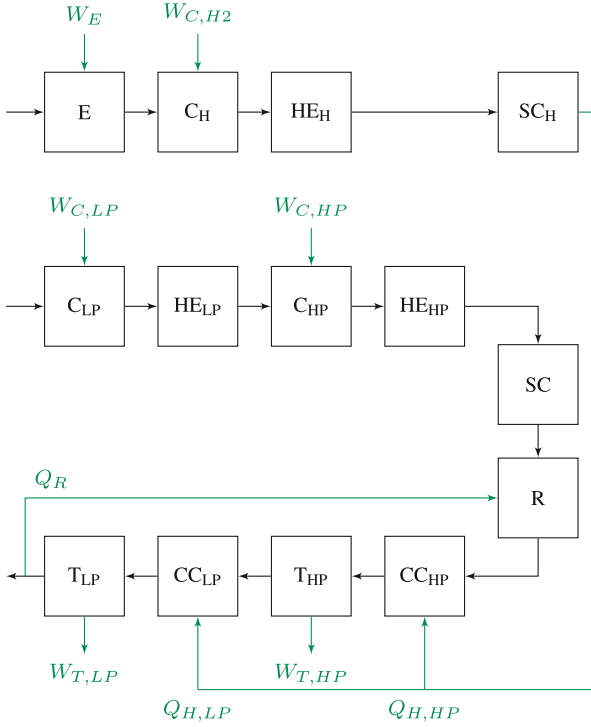
Fig. 9. Block diagram of a hydrogen compressed air energy storage power plant (HCAES), E - electrolysis, C - compressor, HE - heat exchanger, SC - salt cavern, R - recuperation, CC - combustion chamber, T - turbine, LP - low pressure, HP - high pressure.

of the cavern is predefined analogue to the CAES. The input temperature of the compressor corresponds to the operating temperature of the electrolysis. The work of the hydrogen compressors is calculated analogously to the compression of compressed air (Eq. 8 to 11). However, during a complete charging cycle of the compressed air storage, the hydrogen storage is only filled to a fraction. For simplification, it is assumed that $p_{min,H}$ corresponds to the mean pressure in the cavern.

$$W_{C,H} = \int_{p_{min,H}}^{p_{max,H}} \mathrm{d}W_{C,H} \tag{28}$$

$$p_{max,H} = \frac{m_{H,ch} \cdot R_H \cdot \kappa \cdot T_{SC,in}}{V_H} + p_{min,H} \tag{29}$$

The round-trip efficiency of the HCAES is thus:

$$\eta_{HCAES} = \frac{W_T}{|W_{C,A}| + W_E + |W_{C,H}|}. \tag{30}$$
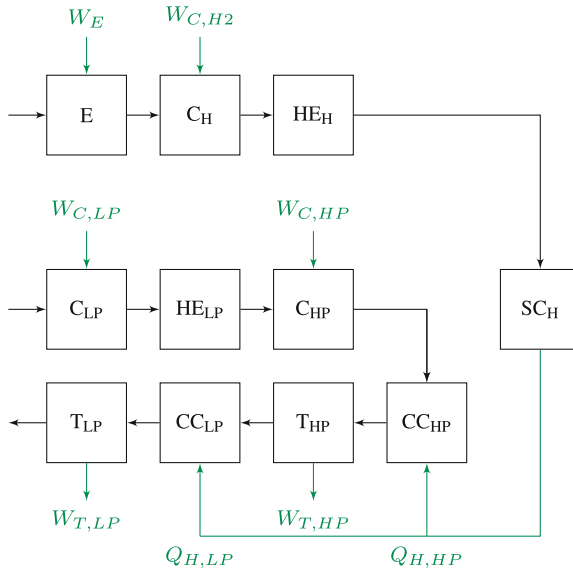
Fig. 10. Block diagram of a hydrogen energy storage power plant with a gas turbine (HES-GT), E - electrolysis, C - compressor, HE - heat exchanger, SC - salt cavern, CC - combustion chamber, T - turbine, LP - low pressure, HP - high pressure.

HES-GT: The block diagram of the hydrogen energy storage concept with a gas turbine is shown in Fig. 10.

For both HES concepts, the hydrogen storage is fully charged during one charging cycle. The mass of hydrogen and the work of the electrolysis in charging mode equal:

$$m_{H,ch} = \frac{(p_{max} - p_{min}) \, V_H}{R_H \cdot \kappa \cdot T_{SK,ein}} \tag{31}$$

$$W_E = \frac{m_{H,ch} \cdot LHV_H}{\eta_E}. \tag{32}$$

The work of the hydrogen compressor is calculated analogously to the HCAES. But in contrast to the HCAES, the hydrogen cavern is completely filled within one charging cycle in the HES. For this reason, the limits of the integrals correspond to the minimum and maximum operating pressure of the cavern. Equations 8 to 11 apply.

The mass of hydrogen during discharging mode is used to determine the amount of heat the hydrogen can deliver during discharging mode based on the lower heating value.

$$Q_H = m_{H,dch} \cdot LHV_H \tag{33}$$

$$m_{H,dch} = \frac{V_H}{R_H} \cdot \left(\frac{p_{min}}{T_{SC,min,dch}} + \frac{p_{max} - p_{min}}{\kappa \cdot T_{SC,ein}} \right)$$
$$\cdot \left(1 - \left(\frac{p_{min}}{p_{max}} \right)^{\frac{1}{\kappa}} \right) \tag{34}$$

$$T_{SC,min,dch} = T_{SC,max,dch} \cdot \left(\frac{p_{max}}{p_{min}} \right)^{\left(\frac{\kappa - 1}{\kappa} \right)} \tag{35}$$

In classical gas turbine power plants, the turbine inlet temperatures are between $1000\,°C$ and $1500\,°C$ because the combustion air is not cooled to store in the salt cavern as in the CAES [27]. For this reason, the turbine inlet temperatures for the HES-GT are assumed to be $500\,K$ higher than for the compressed air storage power plant. To determine the air demand during discharging mode, the volume-specific fuel demand q_H is calculated. Equation 9 to 11 and 19 also apply.

$$q_H = \frac{Q_H}{V_A} = \frac{\int_{p_{min}}^{p_{max}} \mathrm{d}Q_{CC,HP} + \int_{p_{min}}^{p_{max}} \mathrm{d}Q_{CC,LP}}{V_A} \tag{36}$$

$$\mathrm{d}Q_{CC,HP} = c_P \cdot (T_{CC,HP,aus} - T_{CC,HP,ein})\, \mathrm{d}m_{A,dch}$$
$$= c_P \cdot (T_{T,HP,ein} - T_{C,HP,aus})\, \mathrm{d}m_{A,dch} \tag{37}$$

$$V_A = \frac{Q_H}{q_H} = \frac{m_{H,dch} \cdot LHV_H}{q_H} \tag{38}$$

The work required to compress the air $(W_{C,A})$ is calculated using Eq. 6 to 11. The work that is recovered during the expansion of the air in the two turbines (W_T) is determined using Eq. 12 to 17.

The round-trip efficiency of the HES-GT equals the work of the turbine minus the work of the air compressor divided by the sum of the work of the electrolysis and the work of the hydrogen compressor.

$$\eta_{HES-GT} = \frac{W_T - |W_{C,A}|}{W_E + |W_{C,H}|} \tag{39}$$

HES-FC: Figure 11 shows the block diagram of the hydrogen energy storage concept with a fuel cell.

The work of the electrolysis and the hydrogen compression in charging mode is calculated analogously to HES-GT. In discharging mode, the amount of hydrogen available is determined using Eq. 34. For the work that is recovered in the fuel cell, the following equation applies.

$$W_{FC} = m_{H,dch} \cdot LHV_H \cdot \eta_{FC} \tag{40}$$

The round-trip efficiency of the HES-FC is calculated with:

$$\eta_{HES-FC} = \frac{W_{FC}}{W_E + |W_{C,H}|}. \tag{41}$$
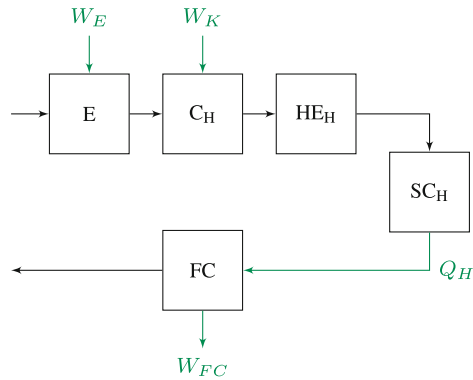
Fig. 11. Block diagram of a hydrogen energy storage power plant with a fuel cell (HES-FC), E - electrolysis, C - compressor, HE - heat exchanger, SC - salt cavern, FC - fuel cell.

References

1. Agora Energiewende. *Electricity Storage in the German Energy Transition.* Study. Berlin, Dec. 2014.
2. Prognos, Ö ko-Institut, and Wuppertal-Institut. *Towards a Climate-Neutral Germany. Executive Summary conducted for Agora Energiewende, Agora Verkehrswende and Stiftung Klimaneutralität.* Study. June 11, 2021.
3. Michael Sterner and Ingo Stadler, eds. *Handbook of Energy Storage: Demand, Technologies, Integration.* Berlin, Heidelberg: Springer Berlin Heidelberg, 2019. ISBN: 978-3-662-55503-3 978-3-662-55504-0. https://doi.org/10.1007/978-3-662-55504-0. URL: http://link.springer.com/10.1007/978-3-662-55504-0 (visited on 12/12/2022).
4. Florian Klumpp. "Comparison of pumped hydro, hydrogen storage and compressed air energy storage for integrating high shares of renewable energies- Potential, cost-comparison and ranking". In: *Journal of Energy Storage* 8 (Sept. 26, 2016), pp. 119-128. ISSN: 2352152X. https://doi.org/10.1016/j.est.2016.09.012
5. Herib Blanco and André Faaij. "A review at the role of storage in energy systems with a focus on Power to Gas and long-term storage". In: *Renewable and Sustainable Energy Reviews* 81 (July 26, 2017), pp. 1049–1086. ISSN: 13640321. https://doi.org/10.1016/j.rser.2017.07.062.
6. Yanjuan Yu, Hongkun Chen, and Lei Chen. "Comparative Study of Electric Energy Storages and Thermal Energy Auxiliaries for Improving Wind Power Integration in the Cogeneration System". In: *Energies* 11.2 (Jan. 23, 2018), p. 263. https://doi.org/10.3390/en11020263.
7. Manal AlShafi and Yusuf Bicer. "Thermodynamic performance comparison of various energy storage systems from source-to-electricity for renewable energy resources". In: *Energy* 219 (Dec. 16, 2020), p. 119626. https://doi.org/10.1016/j.energy.2020.119626
8. Oliver Schmidt et al. "Projecting the Future Levelized Cost of Electricity Storage Technologies". In: *Joule* 3.1 (Jan. 16, 2019), pp. 81–100. ISSN: 25424351. https://doi.org/10.1016/j.joule.2018.12.008.

9. Behnam Zakeri and Sanna Syri. "Electrical energy storage systems: A comparative life cycle cost analysis". In: *Renewable and Sustainable Energy Reviews* 42 (Feb. 1, 2015), pp. 569–596. ISSN: 13640321. https://doi.org/10.1016/j.rser.2014.10.011.

10. Alfonso Arias Pérez and Thomas Vogt. "Life cycle assessment of conversion processes for the large-scale underground storage of electricity from renewables in Europe". In: *EPJ Web of Conferences* 79 (Jan. 1, 2014), p. 03006. https://doi.org/10.1051/epjconf/20137903006.

11. Clemens Mostert et al. "Comparing Electrical Energy Storage Technologies Regarding Their Material and Carbon Footprint". In: *Energies* 11.12 (Dec. 3, 2018), p. 3386. https://doi.org/10.3390/en11123386.

12. Davide Astiaso Garcia et al. "Expert Opinion Analysis on Renewable Hydrogen Storage Systems Potential in Europe". In: *Energies* 9.11 (Nov. 18, 2016), p. 963. https://doi.org/10.3390/en9110963.

13. Marcus Budt et al. "A review on compressed air energy storage: Basic principles, past milestones and recent developments". In: *Applied Energy* 170 (Feb. 20, 2016), pp. 250–268. ISSN: 03062619. https://doi.org/10.1016/j.apenergy.2016.02.108.

14. Xing Luo et al. "Overview of Current Development in Compressed Air Energy Storage Technology". In: *Energy Procedia* 62 (Jan. 1, 2014), pp. 603-611. ISSN: 18766102. https://doi.org/10.1016/j.egypro.2014.12.423.

15. Ibrahim Nabil, Mohamed Mohamed Khairat Dawood, and Tamer Nabil. "Review of Energy Storage Technologies for Compressed-Air Energy Storage". In: *American Journal of Modern Energy* 4.4 (Aug. 23, 2021), pp. 51-60. https://doi.org/10.11648/j.ajme.20210704.12.

16. Qihui Yu et al. "A review of compressed-air energy storage". In: *Journal of Renewable and Sustainable Energy* 11.4 (Aug. 12, 2019), p. 042702. https://doi.org/10.1063/1.5095969.

17. Hossein Safaei and Michael J. Aziz. "Thermodynamic Analysis of Three Compressed Air Energy Storage Systems: Conventional, Adiabatic, and Hydrogen-Fueled". In: *Energies* 10.7 (July 18, 2017), p. 1020. https://doi.org/10.3390/en10071020.

18. Edward R. Barbour, Daniel L. Pottie, and Philip Eames. "Why is adiabatic compressed air energy storage yet to become a viable energy storage option?" In: *iScience* 24.5 (May 21, 2021), p. 102440. ISSN: 25890042. https://doi.org/10.1016/j.isci.2021.102440.

19. European Commission (Directorate General for Energy) et al. *Study on energy storage: contribution to the security of the electricity supply in Europe.* LU: Publications Office, 2020. URL: https://data.europa.eu/doi/10.2833/077257.

20. Friederike Kaiser. "Thermodynamic Steady-State Analysis and Comparison of Compressed Air Energy Storage (CAES) Concepts". In: *International Journal of Thermodynamics* 21.3 (Sept. 1, 2018), pp. 144-156. ISSN: 1301-9724. https://doi.org/10.5541/ijot.407824.

21. S. Eckroad et al. *EPRI-DOE Handbook of Energy Storage for Transmission and Distribution Applications: Final Report.* Abschlussbericht. Palo Alto: EPRI und U.S. Department of Energy, Dec. 2003.

22. D. R. Hounslow et al. "The Development of a Combustion System for a 110 MW CAES Plant". In: *Journal of Engineering for Gas Turbines and Power* 120.4 (Dec. 1998), pp. 875–883. ISSN: 0742–4795, 1528–8919. https://doi.org/10.1115/1.2818482.

23. Chris Bullough et al. "Advanced Adiabatic Compressed Air Energy Storage for the Integration of Wind Energy". In: Proceedings of the European Wind Energy Conference. London, UK, Nov. 22, 2004.

24. Ann-Kathrin Klaas and Hans-Peter Beck. "A MILP Model for Revenue Optimization of a Compressed Air Energy Storage Plant with Electrolysis". In: *Energies* 14.20 (Oct. 18, 2021), p. 6803. https://doi.org/10.3390/en14206803.

25. Alexander Buttler and Hartmut Spliethoff. "Current status of water electrolysis for energy storage, grid balancing and sector coupling via power-togas and power-to-liquids: A review". In: *Renewable and Sustainable Energy Reviews* 82 (Feb. 2018), pp. 2440-2454. ISSN: 13640321. https://doi.org/10.1016/j.rser.2017.09.003.

26. Siemens Energy. *Hydrogen power and heat with Siemens Energy gas turbines.* Report. 2022.

27. Kamal Abudu et al. "Gas turbine efficiency and ramp rate improvement through compressed air injection". In: *Proceedings of the Institution of Mechanical Engineers, Part A: Journal of Power and Energy* 235.4 (June 15, 2020), pp. 866–884. ISSN: 0957–6509, 2041–2967. https://doi.org/10.1177/0957650920932083.

28. Friederike Kaiser. "Steady State and Time Dependent Compressed Air Energy Storage Model Validated with Huntorf Operational Data and Investigation of Hydrogen Options for a Sustainable Energy Supply". PhD thesis. Göttingen: Cuvillier Verlag, July 19, 2020.

29. Jeffrey Goldmeer. *Power to Gas: Hydrogen for Power Generation: Fuel Flexible Gas Turbines as Enablers for a Low or Reduced Carbon Energy Ecosystem.* Report. Issue: GEA33861. General Electric Company, Feb. 2019.

30. Iain Staffell et al. "The role of hydrogen and fuel cells in the global energy system". In: *Energy & Environmental Science* 12.2 (Dec. 10, 2018), pp. 463–491. ISSN: 1754–5692, 1754–5706. https://doi.org/10.1039/C8EE01157E.

31. Ahmet Ozarslan. "Large-scale hydrogen energy storage in salt caverns". In: *International Journal of Hydrogen Energy* 37.19 (Aug. 11, 2012), pp. 14265-14277. ISSN: 03603199. https://doi.org/10.1016/j.ijhydene.2012.07.111.

32. Fritz Crotogino. "Traditional Bulk Energy Storage- Coal and Underground Natural Gas and Oil Storage". *In: Storing Energy.* 2016, pp. 391–409. https://doi.org/10.1016/B978-0-12-803440-8.00019-1.

33. Olaf Kruck et al. *Overview on all Known Underground Storage Technologies for Hydrogen.* Projektbericht. Hannover, Aug. 14, 2013.

34. Adam Christensen. *Assessment of Hydrogen Production Costs from Electrolysis: United States and Europe.* Study. International Council on Clean Transportation, June 1, 2020.

35. Sven Kreidelmeyer et al. *Kosten und Transformationspfade für strombasierte Energieträger: Studie im Auftrag des Bundesministeriums für Wirtschaft und Energie.* Endbericht. Prognos AG, May 2020.

36. Klaus Stolzenburg et al. *Integration von Wind- Wasserstoff-Systemen in das Energiesystem: Abschlussbericht.* Abschlussbericht. Num Pages: 250. PLANET Planungsgruppe Energie und Technik GbR, Mar. 31, 2014.

37. Gunther Glenk and Stefan Reichelstein. "Economics of converting renewable power to hydrogen". In: *Nature Energy* 4.3 (Feb. 25, 2019), pp. 216–222. https://doi.org/10.1038/s41560-019-0326-1.

38. Luca Bertuccioli et al. *Study on development of water electrolysis in the EU: Final Report.* Final report. E4tech S'arl, Element Energy Ltd, Feb. 2014.

39. Johannes Töpler and Jochen Lehmann, eds. *Wasserstoff und Brennstoffzelle: Technologie und Marktperspektiven.* 2. Auflage. Springer Berlin Heidelberg, 2017. ISBN: 978-3-662-53360-4.

40. Tom Smolinka et al. *Studie IndWEDe: Industrialisierung der Wasserelektrolyse in Deutschland: Changen und Herausforderungen für nachhaltigen Wasserstoff für Verkehr, Strom und Wärme.* Berlin: NOW GmbH, 2018.

41. Prognos, Öko-Institut, and Wuppertal-Institut. *Klimaneutrales Deutschland: Studie im Auftrag von Agora Energiewende, Agora Verkehrswende und Stiftung Klimaneutralität.* Berlin, Nov. 2020.

42. International Energy Agency. *The Future of Hydrogen.* Japan, June 2019.

43. Manish Kumar Singla, Parag Nijhawan, and Amandeep Singh Oberoi. "Hydrogen fuel and fuel cell technology for cleaner future: a review". In: *Environmental Science and Pollution Research* 28.13 (Apr. 2021), pp. 15607–15626. https://doi.org/10.1007/s11356-020-12231-8.

44. Milhilesh Kumar Sahu and Sanjay. "Comparative exergoeconomics of power utilities: Air-cooled gas turbine cycle and combined cycle configurations". In: *Energy* 139 (Nov. 15, 2017), pp. 42–51. https://doi.org/10.1016/j.energy.2017.07.131.

45. Behzad Najafi et al. "Exergetic, economic and environmental analyses and multi-objective optimization of an SOFC-gas turbine hybrid cycle coupled with an MSF desalination system". In: *Desalination* 334.1 (Feb. 3, 2014), pp. 46–59. https://doi.org/10.1016/j.desal.2013.11.039.

46. Anna S. Lord, Peter H. Kobos, and David J. Borns. "Geologic storage of hydrogen: Scaling up to meet city transportation demands". In: *International Journal of Hydrogen Energy* 39.28 (Sept. 2014), pp. 15570–15582. ISSN: 03603199. https://doi.org/10.1016/j.ijhydene.2014.07.121. (Visited on 12/06/2022).

47. Heinz Herwig. *Wärmeübertragung A-Z.* Berlin, Heidelberg: Springer Berlin Heidelberg, 2000. ISBN: 978-3-642-63106-1

48. R. Ray et al. *Hydrogen Storage and Flexible Turbine Systems WP2 Report - Hydrogen Storage.* energy technologies institute, July 29, 2013.

49. Antje Seitz, Stefan Zunft, and Carsten Hoyer-Klick. *Technologiebericht 3.3b Energiespeicher (thermisch, thermo-chemisch und mechanisch) innerhalb des Forschungsprojekts TF_Energiewende.* Deutsches Zentrum für Luftund Raumfahrt e.V., Mar. 29, 2018.

50. Paul Rundel et al. *Speicher für die Energiewende. Studie.* Sulzbach-Rosenberg: Fraunhofer-Institut für Umwelt-, Sicherheits- und Energietechnik UMSICHT, Sept. 2019

51. Christoph Noack et al. *Studie über die Planung einer Demonstrationsanlage zur Wasserstoff-Kraftstoffgewinnung durch Elektrolyse mit Zwischenspeicherung in Salzkavernen unter Druck.* Studie. Stuttgart: Deutsches Zentrum für Luftund Raumfahrt, Feb. 5, 2015. https://doi.org/10.2314/GBV:824812212.

52. Martin Zapf. *Stromspeicher und Power-to-Gas im deutschen Energiesystem: Rahmenbedingungen, Bedarf und Einsatzmöglichkeiten.* https://doi.org/10.1007/978-3-658-15073-0. Mönchsberg: Springer, Berlin Heidelberg, Jan. 1, 2017. ISBN: 978-3-658-15073-0.

53. Ulrich Fischer et al. *Wissenschaftliche Forschung zu Windwasserstoff-Energiespeichern - WESpe.* Schlussbericht. Cottbus, Dec. 31, 2017. https://doi.org/10.2314/GBV:1032718846.

54. Dimitris K. Niakolas et al. "Fuel cells are a commercially viable alternative for the production of "clean" energy". In: *Ambio* 45 (S1 Dec. 14, 2015), pp. 32-37. https://doi.org/10.1007/s13280-015-0731-z.

55. International Energy Agency. *Technology Roadmap: Hydrogen and Fuel Cells.* Paris, 2015.

56. Akbar Maleki and Alireza Askarzadeh. "Comparative study of artificial intelligence techniques for sizing of a hydrogen-based stand-alone photovoltaic/ wind hybrid system". In: *International Journal of Hydrogen Energy* 39.19 (June 2014), pp. 9973-9984. https://doi.org/10.1016/j.ijhydene.2014.04.147.

57. Abolfazl Shiroudi and Seyed Reza Hosseini Taklimi. "Demonstration Project of the Solar Hydrogen Energy System Located on Taleghan-Iran: Technical-Economic Assessments". In: World Renewable Energy Congress - Sweden, 8–13 May, 2011, Linköping, Sweden. Nov. 3, 2011, pp. 1158–1165. https://doi.org/10.3384/ecp110571158.

58. Yvonne Ruf et al. "Development of Business Cases for Fuel Cells and Hydrogen Applications for Regions and Cities". Brüssel, 2017.

59. Friederike Kaiser and Uwe Krüger. "Exergy analysis and assessment of performance criteria for compressed air energy storage concepts". In: International Journal of Exergy 28.3 (Jan. 1, 2019). Number Of Volumes: 10020032, p. 229. ISSN: 1742–8297. https://doi.org/10.1504/IJEX.2019.10020032.

60. European Commission. HORIZON 2020 - Work Programme 2014–2015: 19. General Annexes. Dec. 4, 2015. (Visited on 03/25/2022).

61. Edward Barbour and Daniel L. Pottie. "Adiabatic compressed air energy storage technology". In: Joule 5.8 (Aug. 2021), pp. 1914–1920. ISSN: 25424351. https://doi.org/10.1016/j.joule.2021.07.009. (Visited on 08/23/2022).

62. Roxanne Pinsky et al. "Comparative review of hydrogen production technologies for nuclear hybrid energy systems". In: Progress in Nuclear Energy 123 (May 2020), p. 103317. https://doi.org/10.1016/j.pnucene.2020.103317. (Visited on 08/23/2022).

63. IEA. Hydrogen project database. Oct. 2021. URL: https://www.iea.org/reports/hydrogen-projectsdatabase

64. IEA. ETP Clean Energy Technology Guide. Nov. 4, 2021. URL: https://www.iea.org/articles/etp-clean-energy-technology-guide

65. Viviana Cigolotti, Matteo Genovese, and Petronilla Fragiacomo. "Comprehensive Review on Fuel Cell Technology for Stationary Applications as Sustainable and Efficient Poly-Generation Energy Systems". In: Energies 14.16 (Aug. 13, 2021), p. 4963. ISSN: 1996-1073. https://doi.org/10.3390/en14164963.

66. Deutsche Energie-Agentur GmbH. dena Ancillary Services Study 2030. Final report. Berlin: German Energy Agency, Oct. 11, 2014.

67. Ivan Calero, Claudio A. Canizares, and Kankar Bhattacharya. "Compressed Air Energy Storage System Modeling for Power System Studies". In: IEEE Transactions on Power Systems 34.5 (Jan. 2019), pp. 3359-3371. ISSN: 0885-8950. https://doi.org/10.1109/TPWRS.2019.2901705.

68. Pan Zhao et al. "A preliminary dynamic behaviors analysis of a hybrid energy storage system based on adiabatic compressed air energy storage and flywheel energy storage system for wind power application". In: Energy 84 (May 2015), pp. 825–839. ISSN: 03605442. https://doi.org/10.1016/j.energy.2015.03.067. (Visited on 03/22/2022).

69. Hans-Peter Beck et al. Eignung von Speichertechnologien zum Erhalt der Systemsicherheit. Studie. Goslar: Energie-Forschungszentrum Niedersachsen, Mar. 8, 2013.

70. Wenju Sang et al. "Virtual Synchronous Generator, a Comprehensive Overview". In: Energies 15.17 (Aug. 24, 2022), p. 6148. ISSN: 1996-1073. https://doi.org/10.3390/en15176148. URL: https://www.mdpi.com/1996-1073/15/17/6148(visitedon12/28/2022).

71. Adriano Sciacovelli et al. "Dynamic simulation of Adiabatic Compressed Air Energy Storage (A-CAES) plant with integrated thermal storage - Link between components performance and plant performance". In: Applied Energy 185 (Jan. 2017), pp. 16-28. ISSN: 03062619. https://doi.org/10.1016/j.apenergy.2016.10.058.

URL: https://linkinghub.elsevier.com/retrieve/pii/S0306261916315021 (visited on 12/14/2022).

72. Siddhartha Kumar Khaitan and Mandhapati Raju. "Dynamics of hydrogen powered CAES based gas turbine plant using sodium alanate storage system". In: *International Journal of Hydrogen Energy* 37.24 (Jan. 1, 2012), pp. 18904-18914. ISSN: 03603199. https://doi.org/10.1016/j.ijhydene.2012.10.004.

73. Lasse Nielsen and Reinhard Leithner. "Dynamic Simulation of an Innovative Compressed Air Energy Storage Plant - Detailed Modelling of the Storage Cavern". In: *WSEAS TRANSACTIONS on POWER SYSTEMS* 8.4 (Aug. 2009). ISSN: 1790–5060.

74. IRENA. *Hydrogen: A renewable energy perspective.* Abu Dhabi: International Renewable Energy Agency, Sept. 2019.

75. Ahmad Mayyas and Margaret Mann. "Emerging Manufacturing Technologies for Fuel Cells and Electrolyzers". In: *16th Global Conference on Sustainable Manufacturing - Sustainable Manufacturing for Global Circular Economy.* Vol. 33. 2019, pp. 508-515. https://doi.org/10.1016/j.promfg.2019.04.063.

76. Ann-Kathrin Fries et al. "Huntorf 2020 - Improvement of Flexibility and Efficiency of a Compressed Air Energy Storage Plant based on Synthetic Hydrogen". In: *NEIS 2018; Conference on Sustainable Energy Supply and Energy Storage Systems.* NEIS 2018; Conference on Sustainable Energy Supply and Energy Storage Systems. Sept. 2018, pp. 1–5.

77. Fritz Crotogino et al. "Large-Scale Hydrogen Underground Storage for Securing Future Energy Supplies". In: *18th World Hydrogen Energy Conference 2010.* Ed. by Detlef Stolten and Thomas Grube. Vol. 78–4. Schriften des Forschungszentrums Jülich / Energy & Environment. May 16, 2010. ISBN: 978-3-89336-654-5.

78. Janusz Kotowicz, Mateusz Brzeczek, and Marcin Job. "The thermodynamic and economic characteristics of the modern combined cycle power plant with gas turbine steam cooling". In: *Energy* 164 (Aug. 11, 2018). Num Pages: 18, pp. 359-376. ISSN: 03605442. https://doi.org/10.1016/j.energy.2018.08.076.

79. A. G. Olabi et al. "Compressed air energy storage systems: Components and operating parameters - A review". In: *Journal of Energy Storage* 34 (Feb. 2021). https://doi.org/10.1016/j.est.2020.102000.